A Robotic GPR Pipeline for Automated Subsurface Analysis in Multiple Scenarios

Nuria Rodríguez Calderón[1(✉)], Berta Viñes Santamaria[1], David Caballero Flores[1], Tahzeeb Hussain[1], and Vega Perez-Gracia[2]

[1] Centre de Disseny d'Equips Industrials (CDEI), Universitat Politècnica de Catalunya, Barcelona, Spain
nuria.rodriguez.calderon@upc.edu

[2] Universitat Politècnica de Catalunya-BarcelonaTech. Dpt. Resistència de Materials i Estructures a l'Enginyeria. Escola d'Enginyeria de Barcelona Est., Barcelona, Spain

Abstract. GPR is a technique for shallow subsurface sensing, but its use is limited by variable acquisition conditions and labor-intensive interpretation. This work presents a robotic GPR pipeline for agricultural and construction scenarios, combining two complementary sensing platforms with automated radargram processing. The framework includes radargram standardization, AI-based hyperbola detection, geometric fitting, circular slice generation, and frequency-domain analysis. Results show root density related patterns, as well as discrimination between metallic and plastic pipes. Additional branches for soil-moisture estimation and material classification are under development.

Keywords: Ground-penetrating radar (GPR) · robotic surveying · hyperbola detection · subsurface analysis

1 Introduction

Ground-penetrating radar (GPR) is a non-destructive electromagnetic technique for shallow subsurface investigation, as it enables the detection of buried structures and material interfaces through contrasts in dielectric properties [6]. It operates by emitting short pulses into the material and recording the reflections generated when the waves encounter discontinuities. These reflections are registered over time to form radargrams, in which two main feature types are typically observed: hyperbolic signatures, associated with localized buried objects detected as the antenna passes over them (e.g., reinforcement bars, pipes, or voids), and horizontal reflections, which indicate layer boundaries or changes in material composition.

Despite its potential, practical GPR use remains limited by operator-dependent acquisition and labor-intensive interpretation. Survey quality is sensitive to acquisition conditions, while radargrams often require expert preprocessing and manual inspection. To address both issues, this work proposes a

© The Author(s), under exclusive license to Springer Nature Switzerland AG 2027
O. Gervasi et al. (Eds.): ICCSA 2026 Workshops, LNCS 16766, pp. 393–404, 2027.
https://doi.org/10.1007/978-3-032-30539-8_31

robotic GPR framework that combines repeatable acquisition with automated radargram processing for agricultural and construction scenarios.

2 Related Work

GPR has been extensively studied for subsurface characterization, with applications spanning the detection of underground utilities [18], assessment of infrastructure condition [14], soil mapping and moisture estimation [12]. However, the effectiveness of these applications strongly depends on the consistency of data acquisition. To improve the repeatability and scalability of GPR surveys, recent research has focused on integrating GPR sensors into robotic platforms [8]. Most robotic GPR systems rely on ground mobile platforms to ensure stable antennaground coupling. Other configurations have been also explored: crawler-based where manual access is difficult [3], in-pipe robots for internal inspection of underground structures, and UAV-based robotic systems [11]. Despite these advances, robotic GPR systems remain limited by localization challenges (especially in GNSS-denied environments) and difficulties in maintaining consistent acquisition conditions.

In parallel, to address radargram interpretation challenges, research has focused on automated and semi-automated methods based on signal processing and machine learning. More recently, deep learning methods have demonstrated strong performance in tasks such as hyperbola detection and GPR denoising [1], enabling more scalable interpretation pipelines. Nevertheless, their performance remains limited by data scarcity and domain generalization issues [17].

However, these two research directions (robotic data acquisition and automated interpretation) have largely evolved independently, highlighting the need for integrated frameworks that jointly address both aspects.

3 Robotic Platforms and GPR Sensing System

The overall approach is conceived as a GPR-centred system in which robotic platforms act as acquisition enablers and the downstream processing chain transforms radar measurements into application-relevant information. To accommodate different operational requirements, the framework relies on two complementary robotic platforms (Fig. 1). Agromoby [5] is designed for agricultural and field environments, where large-area coverage, uneven terrain, and stable ground-following acquisition are essential. The platform is coupled with MALÅ impulse GPR antennas with single-frequency configurations ranging from 200 to 2500 MHz, allowing the operating frequency to be selected according to the required trade-off between penetration depth and spatial resolution. The antenna is mounted on an external non-conductive support with a passive wheel to maintain a near-constant antenna-ground distance.

In contrast, Oliwall [7] is conceived for demolition scenarios, where sensing must cover horizontal and elevated structures. The platform integrates a compact multi-frequency GPR system, the Screening Eagle Proceq GP8800, suited to

short-range, very-high-resolution inspection tasks such as reinforcement bars or internal structural features. The sensor is mounted on a robotic manipulator combined with an elevation column, enabling inspection of overhead surfaces up to approximately 2.8 m.

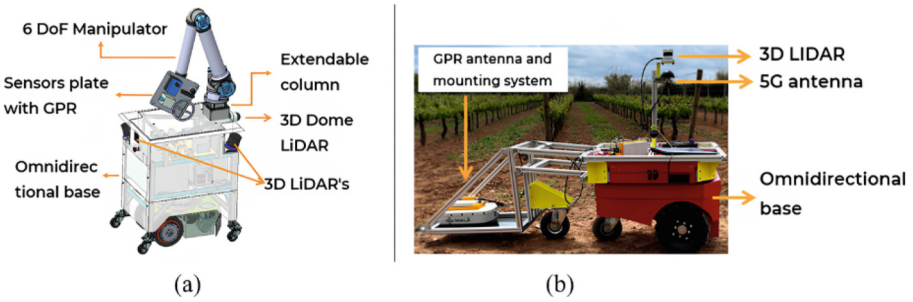

Fig. 1. Robotic platforms for GPR sensing: (a) OLIWALL, a mobile manipulator with arm-mounted GPR for structural inspection; (b) AGROMOBY, an agricultural robot with ground-supported GPR for field surveys.

From a motion-control perspective, both platforms ensure repeatable and structured scanning trajectories. The current acquisition strategy does not rely on a conventional wheel-based GPR odometer; instead, trace positioning combines time-based acquisition, electronic odometry, and robot localization under approximately constant-speed motion. In AGROMOBY, ROS2-based navigation fuses LiDAR, GNSS, IMU, and vision for autonomous field traversal under consistent sampling conditions, with the antenna operated in a near-contact configuration and an air gap kept below approximately 20 cm; larger stand-off distances reduce antenna coupling. In OLIWALL, the target configuration is contact acquisition against the inspected surface, and a non-wheel, contact-based mechanical odometer is under design. In both cases, robotic–GPR integration is handled through ROS2 interfaces; for the Proceq GP8800, communication additionally relies on the manufacturer's API.

Despite these capabilities, several practical challenges remain. Mechanical vibrations can introduce radar noise, maintaining a consistent antenna–surface distance is non-trivial, localization errors directly affect spatial interpretation, and electromagnetic interference from onboard electronics must be minimized. These issues highlight the importance of co-design between the robotic platform and the sensing system to ensure reliable GPR acquisition. The final outputs of the framework, as well as the specific interpretation pathway used to obtain them, depend on the target application. In construction scenarios, the system supports the detection and characterization of hidden structural elements and material contrasts, whereas in agricultural contexts it is oriented toward root-related analysis and soil-moisture-related variability.

4 GPR Data Processing and Interpretation

Once acquired, the data is converted into radargrams, which form the common input to the interpretation pipeline. As shown in Fig. 2, this pipeline combines a shared backbone with application-specific branches.

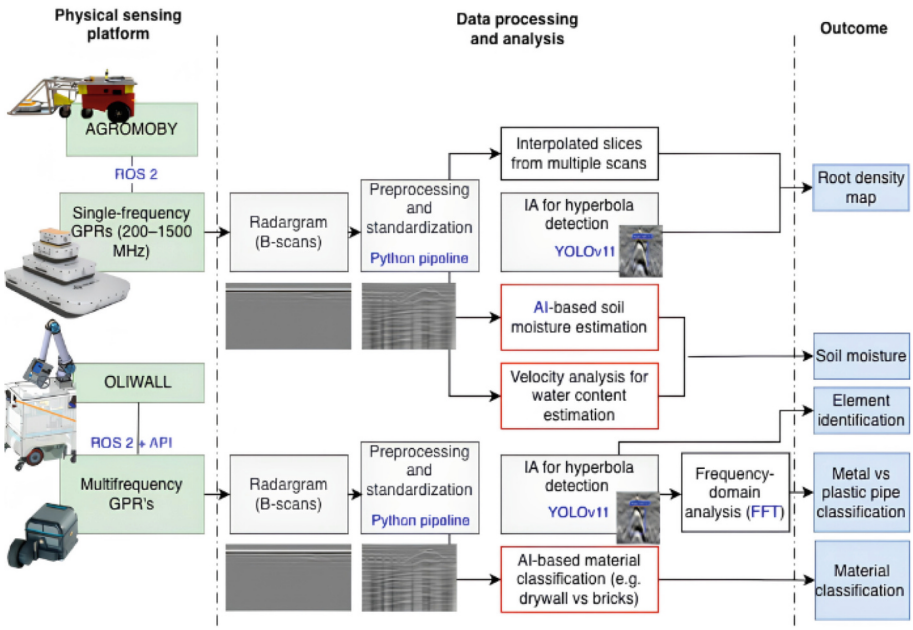

Fig. 2. Robotic GPR framework. Red: work in progress; grey: shared stages. (Color figure online)

4.1 Radargram Preprocessing and Standardization

Radargram standardization is essential for automated GPR interpretation. In conventional practice, visualization and preprocessing are often adjusted manually in commercial software such as `Reflex` or `GPR-SLICE`, which is not compatible with a robotic pipeline. In the present work, radargrams are standardized using basic metadata, including the number of traces and samples, from which an aspect ratio is defined automatically. Although formally a visualization choice, this becomes an important step when radargrams are used as inputs for automated analysis, particularly in image-based AI pipelines. A shared preprocessing sequence is then applied to all radargrams within the same application-specific outcome, based on prior expert knowledge. The current implementation uses automatic time-zero correction, background removal, dewow, low-frequency suppression, and linear gain within a Python workflow integrated into the ROS-based processing pipeline.

4.2 AI-Based Detection of Subsurface Hyperbolas

Deep learning techniques have been increasingly adopted for the automated detection of subsurface objects from GPR data in engineering and environmental applications [17]. As discussed previously, GPR radargrams typically contain two main types of signatures: hyperbolas, associated with localized buried objects, and horizontal reflections, associated with layer boundaries. Most automated interpretation efforts have focused on hyperbola detection, evolving from classical methods such as the Hough transform and template matching [19] toward convolutional neural networks and one-stage object detectors [2]. Among these, the YOLO family has shown strong performance due to its efficiency and accuracy [20], and has already been applied successfully to hyperbola detection and segmentation in GPR B-scans [4,15]. Following this line, the present work adopts YOLOv11M for hyperbola detection. In contrast, the automated interpretation of horizontal reflections remains less mature.

Training a reliable deep learning model requires large annotated datasets, yet acquiring and labelling GPR data is costly and expert-dependent. To mitigate this, the present work uses the publicly available GPR Scans Pipeline dataset from Roboflow Universe [10], containing annotated B-scan images for underground pipeline detection with bounding-box labels of hyperbolic signatures. This dataset is combined with experimental data acquired using the OLIWALL and AGROMOBY platforms. The dataset comprises 1,508 labelled B-scan images, split into training and validation subsets in an 80:20 ratio. YOLOv11M was fine-tuned from pre-trained weights (`yolo11m.pt`) for up to 100 epochs with early stopping and a batch size of 4. The best checkpoint was obtained at epoch 53, and the corresponding validation results are summarized in Table 1.

The balance between precision and recall suggests no pronounced bias toward false positives or negatives. Figure 3 shows representative validation detections. However, transferability to out-of-distribution data remains limited, with lower confidence and more false negatives in new environments. This reflects dataset bias and the current single-class formulation. Improving generalization will require larger, more diverse real datasets, potentially complemented with synthetic data generated with gprMax [21].

Table 1. Validation performance of the fine-tuned YOLOv11M model.

Metric	Value
mAP@50	0.878
mAP@50–95	0.439
Precision	0.855
Recall	0.852

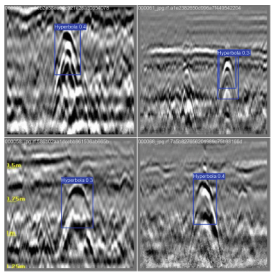

Fig. 3. Hyperbola detections.

4.3 Hyperbola Geometric Fitting: Estimation of Position, Depth and Apparent Size

The output of the AI-based detection stage consists of bounding boxes that localize hyperbolic signatures within the radargram. Since a detection model is used rather than a segmentation approach, these regions of interest do not directly describe the hyperbola geometry. Therefore, the detected regions are mapped back from the image representation to the original numerical GPR data, where each B-scan is treated as an amplitude matrix. Within each region, candidate points are identified as local amplitude maxima and evaluated according to geometric consistency criteria to determine whether they follow a hyperbolic pattern. For the valid points, a hyperbolic fitting procedure is applied using the analytical diffraction model:

$$t(x) = \sqrt{t_0^2 + \frac{4(x - x_0)^2}{v^2}} \tag{1}$$

where x_0 is the horizontal position of the target, t_0 is the two-way travel time at the apex, and v is the propagation velocity in the medium. Once fitted, the hyperbola apex is used to estimate the target position and depth d:

$$d = \frac{v \cdot t_0}{2} \tag{2}$$

The curvature and lateral extent of the fitted curve also provide an approximation of the apparent object size. This estimation requires knowledge, or at least reasonable assumption, of the propagation velocity in the medium. Although not directly known, it can often be approximated from contextual information. In construction scenarios, common materials such as concrete tend to exhibit similar velocity ranges, and OLIWALL provides complementary sensing information that helps select suitable values.

4.4 Frequency-Domain Analysis

This analysis corresponds to an application-specific processing branch aimed at distinguishing between metallic and plastic pipes. While recent studies have explored deep learning and feature-based approaches for material discrimination in GPR data [13], we adopt a simpler initial approach based on a physically interpretable descriptor: the spectral energy of the signal.

Once the hyperbolic signature has been localized through AI-based detection and geometric fitting, the corresponding GPR trace is transformed into the frequency domain using the fast Fourier transform (FFT), and the spectral energy is computed from the FFT magnitude as a comparative feature. The results shown in Fig. 4 are obtained from real experimental data acquired over intentionally buried pipes. Complementary analyses using simulated data generated with gprMax [21] lead to consistent observations. Metallic objects produce significantly higher spectral energy values than plastic ones, due to their higher

conductivity and stronger impedance contrast with the surrounding medium. As shown in Fig. 4, steel and aluminium exhibit clearly higher energy distributions than plastic, indicating that spectral energy is an effective feature for distinguishing metallic from non-metallic targets.

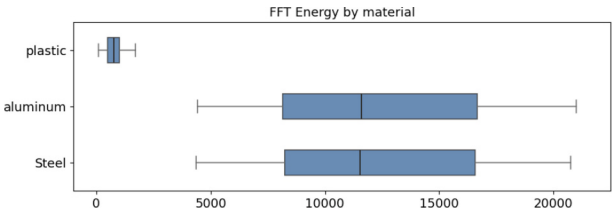

Fig. 4. Distribution of FFT-based spectral energy for different buried pipe materials, from real experimental data.

4.5 Slice-Based Spatial Analysis

Beyond point-wise analysis of individual radargrams, spatial interpretation can be enhanced through the generation of slices, which represent the distribution of signal amplitude at a given depth (or time sample) across multiple scans. These slices provide a planar view of the subsurface response and are particularly useful for identifying spatial patterns and structures that are not evident in single B-scans. In this work, slices are generated directly from the preprocessed GPR data using custom Python tools. While conventional slice generation typically assumes linear survey trajectories, a key contribution of this work is the extension to circular slice representations. This is particularly relevant for acquisition strategies based on circular scanning patterns, where the robot collects data along concentric paths. This choice is motivated by the approximately radial growth of tree roots and has been useful in our root-system analysis (see Sect. 5); similar concentric circular GPR scanning schemes have been used for root-system reconstruction [9].

4.6 Work in Progress Pipelines and Scenarios: Soil Moisture and Material Classification

In addition to the core processing backbone, several application-specific branches are still under development (highlighted in red in Fig. 2) and are therefore presented here as ongoing work rather than consolidated contributions.

One of these lines addresses soil-moisture estimation from GPR data. Since water content affects electromagnetic propagation velocity, classical methods typically require calibration with reflectors or objects buried at known depths [12], making them poorly suited to autonomous robotic operation. Preliminary field tests have therefore been combined with synthetic datasets generated with gprMax [21] to investigate feature correlations with soil water content [22].

Figure 5 presents peak instantaneous amplitude (PIA) as a function of water content, showing linear trends. In parallel, learning-based approaches are being explored, building on previous work by the authors [16], although these models have not yet been integrated into the full pipeline.

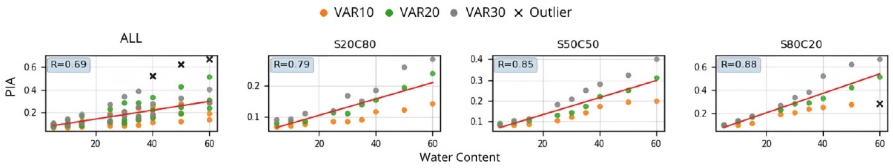

Fig. 5. Example of GPR a feature response (PIA) for 3 heterogeneous synthetic soils. Columns correspond to different sand–clay soil textures,while VAR10, VAR20, and VAR30 indicate water-content variability around the nominal value of ±10%, ±20%, and ±30%.

A second ongoing line focuses on material classification in construction environments, in particular the discrimination between drywall and brick structures using the OLIWALL platform. Preliminary observations suggest that drywall produces more homogeneous radar responses, whereas brick walls exhibit stronger internal variability, as illustrated in Fig. 6.

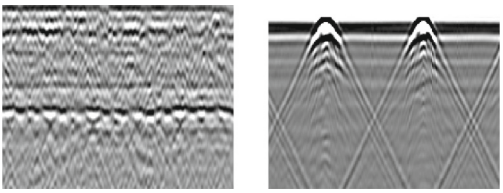

Fig. 6. GPR responses of brick (left) and drywall (right) walls.

5 Experimental Evaluation

The experimental evaluation assesses the proposed processing framework in two representative scenarios. At this stage, data acquisition was performed manually, while following the same sensing configurations and processing pipelines intended for robotic deployment (Fig. 2).

The first experiment addresses root-related signatures in agricultural environments. By comparing excavated root architectures with the corresponding radar responses, large roots are found to produce clear hyperbolic signatures, while additional reflections confirm the non-unique nature of the interpretation. The data was represented as circular slices around the tree, using 10 depth bands between samples 20 and 200 ns and rings with a radial spacing/thickness

of 0.2 m. After standard preprocessing, these slices highlight higher-amplitude zones that correlate with regions of increased root density (Fig. 7), which is often more relevant in practice than exact root reconstruction.

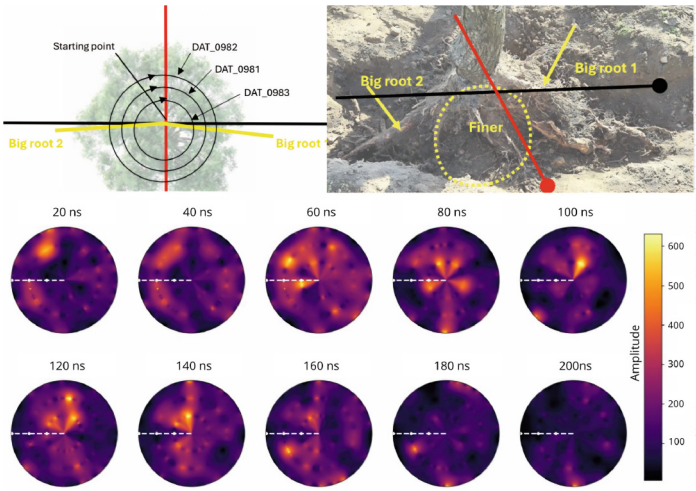

Fig. 7. Comparison between the excavated root layout and circular GPR slices around the tree. The upper panels show the acquisition geometry and excavated roots, while the lower panels show representative amplitude slices. The dashed white line corresponds to the red reference line above. Higher-amplitude regions are spatially consistent with zones of major roots and denser root concentrations. (Color figure online)

The second experiment focuses on material discrimination using buried steel and plastic pipes. Hyperbolas are detected by the AI-based stage, refined by geometric fitting, and analyzed in the frequency domain. In Fig. 8, the radargram spans approximately 60 cm, but the spectral analysis is limited to the first 40 cm: the first two hyperbolas correspond to metallic pipes and the next two to plastic

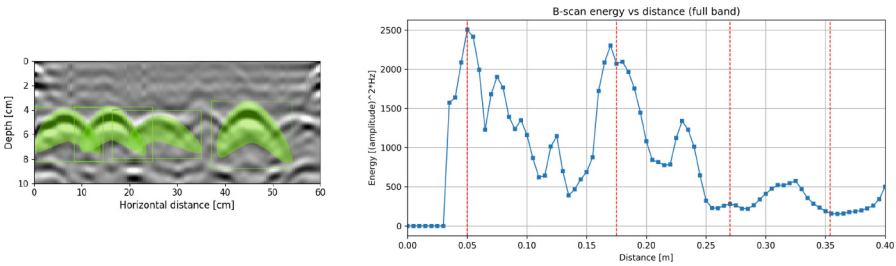

Fig. 8. GPR detections and corresponding energy profile. The radargram extends to 60 cm, while the spectral analysis is limited to the first 40 cm, covering the first four hyperbolas. One plastic target is still poorly detected by the AI model.

pipes, with the last plastic target not detected by the AI model. The remaining detection is not included in the energy profile, as they correspond to another material. The results show that metallic pipes exhibit consistently higher spectral energy than plastic ones, enabling a simple but effective separation.

6 Conclusions and Future Work

The results show that the proposed pipeline is effective for detecting hyperbolic subsurface signatures and supporting application-specific interpretation in different scenarios. In agricultural settings, large roots produce clear hyperbolic responses, while circular slices provide spatial information useful for root density analysis. In controlled construction tests, the combination of AI-based detection, geometric fitting, and frequency-domain analysis enables the estimation of target position and depth, as well as a simple but effective discrimination between metallic and plastic pipes.

More broadly, this work shows that interpretation steps still commonly performed manually can be organized within a robotic GPR framework. Robotic deployment is expected to improve repeatability and coverage, while automated processing reduces the effort required for radargram inspection. At the same time, further automation depends strongly on data availability: some branches already support robust analysis, whereas others still rely on simpler models because larger and more diverse datasets are needed for stronger generalization. This is especially relevant for work-in-progress lines such as soil-moisture estimation and material classification in demolition scenarios.

Future work will focus on full end-to-end robotic deployment. Although the GPR sensors have been integrated with the robotic platforms, the acquisition strategies have not been exploited in real time. The next step is therefore to use the robotic platforms for structured and repeatable scanning, for example in dense root surveys or large wall inspections, and to combine GPR with complementary sensing modalities for more robust and context-aware interpretation.

Acknowledgments. DISCOVER: European Union's Horizon Europe research and innovation programme, grant agreement No. 101129909. ROSAQUA: Government of Catalonia, Agency for the Management of University and Research Grants, Knowledge Industry 2024, grant 2024 PROD 00097. ROOTBOT: Rural Development Program of Catalonia 2014–2022, Department of Climate Action, Food and Rural Agenda, Government of Catalonia.

Disclosure of Interests. The authors have no competing interests.

References

1. Bai, X., et al.: A comprehensive review of conventional and deep learning approaches for ground-penetrating radar detection of raw data. Appl. Sci. **13**(13), 7992 (2023). https://doi.org/10.3390/app13137992

2. Barkataki, N., Tiru, B., Sarma, U.: A CNN model for predicting size of buried objects from GPR B-scans. J. Appl. Geophys. **200**, 104620 (2022). https://doi.org/10.1016/j.jappgeo.2022.104620
3. Bigman, D.P.: Evaluating the feasibility of robotic crawler deployed ground penetrating radar to assess repairs of a concrete hydroelectric dam spillway in Alabama, USA. Water **15**(10), 1858 (2023). https://doi.org/10.3390/w15101858
4. Branco, D., Coutinho, R., Sousa, A., dos Santos, F.: Subsurface metallic object detection using GPR data and YOLOv8-based image segmentation. In: Proceedings of the 21st International Conference on Informatics in Control, Automation and Robotics (ICINCO), pp. 692–699. SciTePress (2024). https://doi.org/10.5220/0013027500003822
5. Caballero, D., et al.: Robotics in sensing the agricultural environment. In: Proceedings of the ASME 2025 International Design Engineering Technical Conferences (IDETC/CIE). Anaheim, CA, USA (2025)
6. Daniels, D.J.: Ground Penetrating Radar. Institution of Engineering and Technology, 2nd edn. (2004)
7. DISCOVER: DISCOVER project, GA 101129909. Horizon Europe Research and Innovation Programme (2024). https://discover-horizon.eu/
8. Eldemiry, A., Muddassir, M., Zayed, T.: Autonomous data acquisition of ground penetrating radar (GPR) using LiDAR-based mobile robot. In: Proceedings of the 41st International Symposium on Automation and Robotics in Construction (ISARC 2024), pp. 206–212. (2024). https://doi.org/10.22260/ISARC2024/0028
9. Fan, G., et al.: 3D reconstruction of root system architecture in urban forest parks based on ground penetrating radar instantaneous amplitude analysis. Plant Phenomics **7**(4), 100147 (2025). https://doi.org/10.1016/j.plaphe.2025.100147
10. GPR Underground Pipeline Detection: GPR scans pipeline dataset. Roboflow Universe (2026). https://universe.roboflow.com/gpr-underground-pipeline-detection/gpr-scans-pipeline. Accessed 18 Apr 2026
11. Halder, S., Afsari, K.: Robots in inspection and monitoring of buildings and infrastructure: a systematic review. Appl. Sci. **13**(4), 2304 (2023). https://doi.org/10.3390/app13042304
12. Huisman, J.A., Hubbard, S.S., Redman, J.D., Annan, A.P.: Measuring soil water content with ground penetrating radar: a review. Vadose Zone J. **2**(4), 476–491 (2003). https://doi.org/10.2136/vzj2003.4760
13. Kalaichelvi, T., Ravi, S., Buddepu, S.: GPR image classification of buried objects using deep learning with attention mechanism. Int. J. Engineering Trends Technol. **73**(4), 24–33 (2025). https://doi.org/10.14445/22315381/IJETT-V73I4P103
14. Lai, W.W.L., Dérobert, X., Annan, A.P.: A review of ground penetrating radar application in civil engineering. NDT & E Int. **96**, 58–78 (2018). https://doi.org/10.1016/j.ndteint.2017.12.006
15. Li, Y., Zhao, Z., Luo, Y., Qiu, Z.: Real-time pattern-recognition of GPR images with YOLO v3 implemented by TensorFlow. Sensors **20**(22), 6476 (2020). https://doi.org/10.3390/s20226476
16. Liso, A., Calderón, N.R., Perez-Gracia, V., D'Orazio, T.R., Renò, V.: Detecting the content of water in agricultural soils by GPR using deep learning. In: Proceedings of SPIE. vol. 13570, p. 3062608 (2024). https://doi.org/10.1117/12.3062608
17. Liu, H., Peng, H., Wang, X., Meng, X., Cui, J., Du, Y.: Comprehensive review of deep learning applications in ground penetrating radar. NDT & E Int. **162**, 103738 (2026). https://doi.org/10.1016/j.ndteint.2026.103738

18. Paul, A., Jayapal, U.M., Ayothiraman, R.: A review of ground penetrating radar for underground utility detection and subsurface profiling: Challenges, strategies and a future-oriented framework. Indian Geotech. J. (2025). https://doi.org/10.1007/s40098-025-01378-1
19. Sagnard, F., Tarel, J.P.: Template-matching based detection of hyperbolas in ground-penetrating radargrams for buried utilities. J. Geophys. Eng. **13**(4), 491–504 (2016). https://doi.org/10.1088/1742-2132/13/4/491
20. Ultralytics: YOLO11 documentation. Online documentation (2024). https://docs.ultralytics.com/models/yolo11/. Accessed 18 Apr 2026
21. Warren, C., Giannopoulos, A., Giannakis, I.: gprMax: open source software to simulate electromagnetic wave propagation for ground penetrating radar. Comput. Phys. Commun. **209**, 163–170 (2016). https://doi.org/10.1016/j.cpc.2016.08.020
22. Zhou, H., et al.: Mapping agricultural soil water content using multi-feature ensemble learning of GPR data. Agricult. Water Manag. **297**, 108884 (2024). https://doi.org/10.1016/j.agwat.2024.108884